Comparative Biochemistry and Physiology, Part A 280 (2023) 111418

Contents lists available at ScienceDirect

Comparative Biochemistry and Physiology, Part A

journal homepage: www.elsevier.com/locate/cbpa

Nitrogen transporters along the intestinal spiral valve of cloudy catshark (*Scyliorhinus torazame*): Rhp2, Rhbg, UT

J. Lisa Hoogenboom [a,*], Marty Kwok-Shing Wong [b], Susumu Hyodo [b], W. Gary Anderson [a]

[a] Department of Biological Sciences, University of Manitoba, Winnipeg, MB R3T 0A8, Canada
[b] Laboratory of Physiology, Atmosphere and Ocean Research Institute, University of Tokyo, Kashiwa, Chiba, Japan

ARTICLE INFO

Editor: Michael Hedrick

Keywords:
Ammonia
Elasmobranch
Kidney
Nitrogen
Ornithine Urea Cycle
Spiral Valve
Transport Protein
Urea

ABSTRACT

As part of their osmoregulatory strategy, marine elasmobranchs retain large quantities of urea to balance the osmotic pressure of the marine environment. The main source of nitrogen used to synthesize urea comes from the digestion and absorption of food across the gastrointestinal tract. In this study we investigated possible mechanisms of nitrogen movement across the spiral valve of the cloudy catshark (*Scyliorhinus torazame*) through the molecular identification of two Rhesus glycoprotein ammonia transporters (Rhp2 and Rhbg) and a urea transporter (UT). We used immunohistochemistry to determine the cellular localizations of Rhp2 and UT. Within the spiral valve, Rhp2 was expressed along the apical brush border membrane, and UT was expressed along the basolateral membrane and the blood vessels. The mRNA abundance of Rhp2 was significantly higher in all regions of the spiral valve of fasted catsharks compared to fed catsharks. The mRNA abundance of UT was significantly higher in the anterior spiral valve of fasted catsharks compared to fed. The mRNA transcript of four ornithine urea cycle (OUC) enzymes were detected along the length of the spiral valve and in the renal tissue, indicating the synthesis of urea via the OUC occurs in these tissues. The presence of Rhp2, Rhbg, and UT along the length of the spiral valve highlights the importance of ammonia and urea movement across the intestinal tissues, and increases our understanding of the mechanisms involved in maintaining whole-body nitrogen homeostasis in the cloudy catshark.

1. Introduction

The osmoregulatory strategy of marine elasmobranchs (sharks, skates, and rays) relies on the synthesis and retention of urea (Smith, 1936). Within shallow-water marine species, such as the cloudy catshark (*Scyliorhinus torazame*), urea can be retained at high concentrations (>300 mM). The nitrogen required to synthesize these large quantities of urea comes from the catabolism of endogenous nitrogenous compounds (e.g. proteins, amino acids) and the intake of exogenous nitrogen, either across the branchial tissues (Wood and Giacomin, 2016), or through the digestion of prey and subsequent uptake across the gastrointestinal (GI) tract (Liew et al., 2013). Investigations into the nitrogen-handling capabilities of the marine elasmobranch GI tract have demonstrated the role of the intestinal spiral valve in the breakdown and bidirectional (influx and efflux) movement of nitrogen (i.e. ammonia and urea; Anderson et al., 2015; Anderson et al., 2010; Bucking, 2015; Hoogenboom et al., 2020; Kajimura et al., 2006; Liew et al., 2013; Wood et al., 2019, 2007, 2005; Wright, 1995).

Ammonia is a product of amino acid, protein, and urea catabolism; however, little is currently known about the movement of ammonia across elasmobranch intestinal tissues, despite the prevalence of ammonia in the spiral valve. Within *in vitro* spiral valve gut sac preparations from North Pacific spiny dogfish (*Squalus acanthias suckleyi*), ammonia concentrations were ~ 1.5 mM in fasted animals, and ~ 4 mM in fed animals (Hoogenboom et al., 2020; Wood et al., 2019). One possible method of ammonia transport across the intestinal tissues may be Rhesus (Rh)-associated glycoproteins, which have been shown to have a direct role in ammonia transport (Marini et al., 2000). The mRNA transcript of several isoforms (Rhag, Rhbg, Rhcg, and Rhp2) have been identified within elasmobranch tissues. In *S. a. suckleyi*, Rhag was identified in the red blood cells, and Rhbg and Rhp2 within the brain, gill, kidney, liver, muscle, rectal gland, cardiac and pyloric stomachs, and spiral valve (Nawata et al., 2015a, 2015b). Rhbg has also been identified within rectal gland, renal tissue, and spiral valve of the little skate (*Leucoraja erinacea*) (Anderson et al., 2010), and Rhcg within gill and renal tissue of the Atlantic spiny dogfish (*Squalus acanthias*)

* Corresponding author.
E-mail address: lisa.hoogenboom@umanitoba.ca (J.L. Hoogenboom).

https://doi.org/10.1016/j.cbpa.2023.111418
Received 25 January 2023; Received in revised form 16 March 2023; Accepted 21 March 2023
Available online 23 March 2023

(Lawrence, 2014). In Japanese banded houndsharks (*Triakis scyllium*), Rhp2 was localized on the basolateral membrane of the renal tubule and was functionally characterized to transport ^{14}C-methylamine (an analog for ammonia) when expressed within *Xenopus* oocytes (Nakada et al., 2010). Despite the ureosmotic and ureotelic nature of marine elasmobranchs, the expression of Rh glycoproteins in various tissues indicates the importance of ammonia trafficking for these animals. Beyond identifying the transcript of these transporters in various elasmobranch tissues, little is currently known about their location and function. Further investigation is necessary to better understand nitrogen metabolism and homeostasis within marine elasmobranchs, and the role of the intestine in nitrogen trafficking in marine elasmobranchs.

As ureosmotic animals, marine elasmobranchs use nitrogen to synthesize urea, primarily via the ornithine urea cycle (OUC) (Schooler et al., 1966). Unlike the mammalian OUC which uses ammonia as the nitrogen-donating substrate, marine elasmobranchs use glutamine, synthesized by glutamine synthetase (GS) transferring nitrogen from ammonia to glutamate (Anderson, 1991; Anderson, 1980). The five additional OUC enzymes are: 1. carbamoyl phosphate synthetase III (CPS III) which is unique to fish and catalyzes the entry of nitrogen (from glutamine) into the cycle, and is likely the rate-limiting enzyme; 2. ornithine transcarbamoylase (OTC); 3. argininosuccinate synthetase (ASS); 4. argininosuccinate lyase (ASL); and, 5. arginase (ARG), which catalyzes the breakdown of arginine to the final products, urea and ornithine (Anderson, 1991). Operating mainly within the liver (Schooler et al., 1966), the enzymes necessary for the OUC to function have also been found in the skeletal muscle and intestinal tissues of *S. a. suckleyi* (Kajimura et al., 2006), the kidney and muscle of the holocephalan elephant shark (*Callorhinchus milii*) (Takagi et al., 2012), and the muscle of the little skate (*Leucoraja erinacea*) (Steele et al., 2005).

To circulate the urea synthesized by the OUC, urea transport (UT) proteins are selective channels that facilitate the controlled diffusion of urea (Shayakul et al., 2013; Shayakul and Hediger, 2004; You et al., 1993). In mammals, there are two known UT classes (UT-A and UT-B) that encode eight isoforms (UT-A1 – A6; UT-B1 – B2) (Shayakul and Hediger, 2004), with an additional class (UT-C) found in teleosts (Mistry et al., 2005). The first UT identified in a marine elasmobranch was shark UT (shUT), a homologue of the mammalian UT-A2 (Smith and Wright, 1999). Expressed within the brain and kidney of *S. a. suckleyi*, shUT was thought to play an osmoregulatory role in the kidney by facilitating reabsorption of urea from the tubule lumen to the blood (Smith and Wright, 1999). To date, UTs have been identified in many elasmobranch tissues, including: brain, gills, liver, kidney, muscle, rectal gland, spiral valve, and testes (Anderson et al., 2010; Hyodo et al., 2004; Janech et al., 2008; Janech et al., 2003; Morgan et al., 2003; Nawata et al., 2015a). In the kidney of the elephant shark, three UT isoforms have been identified along with two variants (efUT-1a, efUT-1b, efUT-2a, efUT-2b, efUT-3); all five transcripts induced a 10-fold increase in ^{14}C-urea uptake when expressed in *Xenopus* oocytes (Kakumura et al., 2009). Within the little skate renal tissue, urea uptake is thought to occur through brush border membrane vesicles by a phloretin-sensitive, non-saturable uniporter in the dorsal section of the kidney, and a phloretin-sensitive, sodium-linked transporter in the ventral section (Morgan et al., 2003). Localized in both the apical and basolateral renal tissue of *T. scyllium*, the *Triakis* UT (tUT) is thought to provide channels for facilitative urea diffusion to reabsorb urea from primary urine in the collecting tubule (Hyodo et al., 2004). Although the mRNA of a UT has been identified within marine elasmobranch spiral valve (Anderson et al., 2010), little is currently known about its localization and function along the GI tract.

The objectives of this study were to investigate the nitrogen-handling capabilities of the cloudy catshark spiral valve through the molecular identification of Rhp2, Rhbg, and UT, and determination of their cellular and tissue localization using immunohistochemistry (IHC) and *in situ* hybridization (ISH). It was hypothesized that the expression of the transport proteins within a tissue would be dependent on the metabolic state of the animal (i.e. access to prandial nitrogen). To examine this, both fed and fasted catsharks were used. Based on the presence of prandial nitrogen available for uptake along the GI tract and the essential role urea plays in osmoregulation for these animals, it was predicted that the expression of the three nitrogen transporters would increase in the fed catsharks compared to the fasted. It was also predicted that the transporters would show increased expression in the posterior region of the spiral valve to facilitate the absorption of nitrogenous compounds as digestion progresses along the length of the intestine. Additionally, the presence of the transcript abundance of four enzymes necessary for the synthesis of urea via the OUC was investigated. It was hypothesized that the metabolic state of the catsharks would affect the mRNA abundance of the enzymes, and it was predicted that all four enzymes would increase following feeding, in an effort to use prandial nitrogen for urea synthesis and whole-body homeostasis.

2. Materials and methods

2.1. Animals and sampling

Male cloudy catsharks obtained from Aqua World Ibaraki Prefectural Oarai Aquarium, Ibaraki, Japan ($n = 12$; 397 ± 7 g) were transferred to the Atmosphere and Ocean Research Institute (AORI), University of Tokyo, Kashiwa, Chiba, Japan. Prior to experimentation, the catsharks were housed and allowed to acclimate for two weeks in 500 L indoor, circular recirculating tanks. Sea water was held at a constant temperature (16.0 ± 1 °C) and salinity (35 ± 1 ppt), and the animals were exposed to 14 h light, 10 h dark photoperiod. Both fed and fasted catsharks were used to compare nitrogen transport during digestion and between meals; food was withheld from the fasted catsharks for 7 days, while the fed catsharks consumed a ration of frozen squid every two days, and were euthanized 24–48 h after feeding.

Catsharks were immersed in a terminal dose of anesthetic (tricaine methanesulfonate, MS-222; 250 ppm; Sigma Aldrich) before a mid-ventral incision was made to expose the abdominal cavity, taking care not to disturb the internal organs. The spiral valve was excised and opened with a longitudinal incision to expose the inner folds. To remove digestive fluids and chyme, the spiral valve was rinsed with elasmobranch Ringer's solution (in mM: urea 400, NaCl 255, TMAO 56, Hepes 10, KCl 6.6, $CaCl_2$ 6.6, $MgCl_2$ 4, $NaHCO_3$ 3.6, $NaSO_4$ 2.4, $NaHPO_4$ 1.4). To reduce the number of animals required for analysis, a longitudinal cut was made down the centre of the spiral valve to separate it into two equal parts (one for determining mRNA abundance and the other for histochemistry). Animal protocols and procedures were approved by the Animal Experiment Committee of the University of Tokyo.

For total RNA extraction, the spiral valve was divided into three regions (anterior, mid, posterior) to examine potential regional differences in transporter expression, as previously described (Anderson et al., 2010); the first two intestinal folds after the pyloric sphincter were classified as anterior, the next two folds were mid folds, and the remaining two folds were posterior. One intestinal fold from each region was removed, frozen immediately in liquid nitrogen and stored at −80 °C. Renal tissue was also excised and handled in the same manner. Intestinal tissues for histological staining were immediately fixed in Bouin's solution (1 part formalin: 3 parts picric acid) at 4 °C for 6 h then transferred to 70% ethanol until analysis.

2.2. RNA isolation

Total RNA was isolated as described previously (Nakada et al., 2010; Yamaguchi et al., 2009). Briefly, tissues were homogenized in Isogen (Nippon Gene, Tokyo, Japan) using a MicroSmash MS-100 (Tomy, Tokyo), and total RNA was extracted according to the manufacturer's protocol. RNA content in the samples was quantified using a nanodrop and 1 μg of total RNA was treated with DNase I (Invitrogen, Thermo Fisher Scientific, Carlsbad, CA, USA) to remove genomic DNA. The DNase-treated RNA was reverse transcribed using the High-Capacity

cDNA Reverse Transcriptase kit according to the manufacturer's protocol (Applied Biosystems, Thermo Fisher Scientific, Foster City, CA, USA).

2.3. Quantification of mRNA abundance by RT-qPCR

The mRNA abundance of three nitrogen transporters (Rhp2, Rhbg, UT) and four OUC enzymes (GS, CPS III, OTC, ARG) within intestinal and renal tissue were quantified using reverse transcription quantitative real-time polymerase chain reaction (RT-qPCR). Primers for the three nitrogen transporter proteins were designed based on genome transcript sequences of cloudy catshark (Hara et al., 2018) (Table 1). Primers for the OUC enzymes were from previously published data (Takagi et al., 2017) (Table 1). RT-qPCR was performed using cDNA transcribed from 1 μg RNA, 1 μM of each respective forward and reverse primer, and KAPA Sybr Fast qPCR kit (Kapa Biosystems) in a 10 μL assay. Standard curves were generated (10^{-2}, 10^{-3}, 10^{-4}, 10^{-5}, 10^{-6}, 10^{-7} ng cDNA) from known quantities of respective purified PCR product (Qiaquick PCR purification kit, Qiagen Inc., Mississauga, ON, Canada). A single PCR product was verified by the melt curve analysis. For relative mRNA abundance, β-actin (ACTB1) was used as the reference gene (Takagi et al., 2017). Suitability for ACTB1 was determined by RT-qPCR having similar expression levels of the gene in all tissues examined (Table S1). To determine target sequences, PCR products were purified using GeneClean III kit (MP Biomedicals, Thomas Scientific) and sequenced using Big Dye Terminator Sequencing kit (Applied Biosystems). Analysis was performed using a Hitachi 3130 Genetic Analyzer (Applied Biosystems). The obtained sequences were confirmed using the basic alignment search tool (BLAST) on the National Center for Biotechnology Information website (NCBI GenBank; http://blast.ncbi.nlm.nih.gov).

2.4. Immunohistochemistry

Antibodies for Rhp2 and UT were previously developed for *T. scyllium* and verified by Western and Northern blotting, and sequencing: Rhp2 (Nakada et al., 2010), and UT (Hyodo et al., 2004). IHC of intestinal tissues were performed as previously described (Hyodo et al., 2004), with the modifications described below. Briefly, intestinal tissues were fixed in Bouin's solution, embedded in paraffin, sectioned (6 μm), and mounted on glass slides (Matsunami Glass). The sections were deparaffinized by xylene, rehydrated in graded ethanol, treated with 0.6% H_2O_2 in methanol for 30 min, washed with deionized water, and incubated in 2% normal goat serum in 10 mM phosphate buffered saline (PBS) containing 0.01% NaN_3 for 60 min. The sections were then incubated in either Rhp2 (1:4000 dilution) or UT (1:2000 dilution) antibody for 1 day at 4 °C within a humidity chamber. Immunoreactive signals were observed using a Vectastain ABC kit (Vector Laboratories, CA) and 3,3′-diaminobenzidine (DAB; ThermoFisher) as the colour reagent according to manufacturer's protocols. Sections were counterstained with hematoxylin after DAB colour development. Negative controls for Rhp2 in the intestinal tissues were performed with the same procedures, but without the primary antibody. To validate the immunohistochemistry of the UT, an immunogen displacement method was used to demonstrate the specific staining from non-specific staining. The UT antiserum was raised against the N-terminal epitope of the banded hound shark UT (Hyodo et al., 2004). To achieve homologous displacement effect, the immunogen peptide (ESEAYQNPFMEKKKT) corresponding to the N-terminal of the catshark UT was custom synthesized (EZBiolab Inc., NJ, USA) for displacement experiments. To displace the specific UT-signals in catshark, 10^{-5} M of the N-terminal peptide was added to the primary antibody incubation to saturate the specific antibody binding sites, but not non-specific binding. As the collecting tubules of kidney were known to contain abundant UT protein, serial kidney sections were included to demonstrate the performance of peptide displacement effect.

Semi-quantitative determination of protein expression was performed for the Rhp2 immunohistochemical staining using *(Fiji is Just) ImageJ* software according to previously published protocols (Crowe et al., 2019; Crowe and Yue, 2019). Ten villi were randomly selected from each spiral valve region (anterior, mid, posterior) for analysis. To account for differences in villi length, DAB staining intensity was normalized by nuclei quantity. Colour deconvolution was used to select for and separate DAB and hematoxylin staining of IHC images: DAB stained images were measured for area of mean grey value; hematoxylin stained images were processed through binary watershed, and analyzed for average nuclei size. Summarized nuclei count was used to divide mean grey value to give an average value of villi staining. Data are presented as a mean ± sem of the ten regional villi.

2.5. In situ hybridization

Tissues were fixed in Bouin's solution, embedded in paraffin, sectioned (6 μm), and mounted on glass slides. The following plasmid DNA (pDNA) templates were used for preparation of digoxigenin (DIG)-labeled riboprobes: a 987-bp fragment of Rhp2, a 972-bp fragment of Rhbg, and a 723-bp fragment of UT. The templates were synthesized from PCR products amplified from specific primers (Table 1) and purified with GENEClean III kit (MP Biomedicals), ligated into a pGEM-T easy vector using Clontech ligation mix (TaKaRa Bio Inc., Japan) with blue/white screening. Insertion of vector was verified by PCR using KAPA Taq EXtra HotStart ReadyMix (Roche, Mannheim, Germany) and sequenced as described above. RNA DIG-labeling kit (T7 sense/SP6 antisense) (Roche) was used on 1 μg purified pDNA (Qiaprep Spin Miniprep kit, Qiagen Inc., Mississauga, ON, Canada) in a 10 μL assay to synthesize DIG-labeled sense and antisense probes.

Hybridization followed a previously published protocol (Takabe et al., 2012), where deparaffinized sections were rehydrated and digested with 30 units of proteinase K (Sigma-Aldrich) in phosphate buffer (PBS) for 10 min at 37 °C. Sections were then treated with 4% paraformaldehyde (PFA; pH 7.4) and active diethyl pyrocarbonate (DEPC; 0.1%), before incubating in pre-hybridization buffer (5× SSC: 0.75 M NaCl and 83.3 mM sodium citrate, pH 7.5; 50% formamide) for 2

Table 1
Primers used in reverse transcription quantitative real-time PCR (RT-qPCR) targeting two Rhesus glycoprotein ammonia transporters (Rhp2, Rhbg), a urea transporter (UT), β-actin (ACTB1), and four OUC enzymes (GS, glutamine synthetase; CPS III, carbamoyl phosphate synthetase III; OTC, ornithine transcarbamylase; ARG, arginase) in cloudy catshark (*Scyliorhinus torazame*).

Gene	Forward primer	Reverse primer	Product size (bp)	Accession no.
	5′ to 3′	5′ to 3′		
Rhp2	GGATCCACATGAGCGTTTA	ACTCGGTGGCAGTGAATATG	150	GCB71145
Rhbg	CCACGTCGAGTGTCGTTAATC	CGAGGGCGTGATCATCATTT	116	AFJ44128
UT	CCGCAACAGGACACTACAA	GAAGCATTGGAGCACTGAGA	102	GCB70015
ACTB1	GCAATCATCTTGATTTTCATGGTACT	CCTGGCARRGCAGACCGTAT	74	LC258081
GS	GAGAGTCAGTCCGCTGCAAGA	CATCAAAATTCCATTCTGGGAGAT	81	LC258078
CPS III	CTCACGATGCGACAGAGATGA	GACAACTGGGTGTTCCTGAGAGA	71	LC258075
OTC	GGGCTTTGAACCAGATTCCA	CATTTTGGTCCCACACTTTTCAG	70	LC258076
ARG	GCTTGGAGGAGACCACAGTTTAG	GAGTGATCCAAGAAAATCCAGG	212	LC258077

h at 58 °C. Sections were incubated overnight in hybridization mixture (same as pre-hybridization buffer) containing thymus DNA and 10–20 ng per slide of DIG-labeled RNA sense or antisense probe (heat denatured at 85 °C for 5 min) at 58 °C. After washing (2× SSC for 30 min at 25 °C, 2× SSC for 60 min at 65 °C, 0.1× SCC for 60 min at 65 °C, and equalization buffer (100 mM Tris-HCL, 150 mM NaCl, pH 7.5) for 5 min at 25 °C), sections were incubated with anti-Digoxigenin-AP Fab Fragments (Roche) (1:5000 dilution in 0.5% Boehinger Blocking reagent provided in DIG nucleic acid detection kit (Roche) for 2 h at 25 °C in a moist chamber. Nitro blue tetrazolium (NBT) and bromochloroindolyl phosphate (BCIP) substrates were used for colour development (Sigma-Aldrich).

2.6. Statistics

Statistical analyses were conducted using *RStudio* (R Core Team, 2017) and Figures were produced using the package *ggplot2* (Wickham, 2009). Data were checked for normality (Shapiro-Wilks) and homogeneity of variance (Levene's test). Two-way analysis of variance (Two-way ANOVA) was performed and Tukey's post hoc test was used to detect significant differences. Differences were accepted as significant when $p < 0.05$. Data are expressed as mean ± sem within the text and Figures.

3. Results

3.1. Rhp2

The effects of metabolic state (fed, fasted) and tissue type (anterior, mid, posterior, kidney) on the mRNA abundance of Rhp2 were analyzed with a two-way ANOVA. There was no significant interaction between the metabolic state and tissue type ($F_{3,35} = 2.3$, $p = 0.1$). For metabolic state, there were significantly higher levels of Rhp2 mRNA in all three spiral valve regions of the fasted catsharks compared to those of the fed ($p < 0.02$) (Fig. 1A). For tissue type, there were no significant differences in mRNA abundance among the tissues of the fasted ($p > 0.3$) and fed (p > 0.3) catsharks.

To determine the cellular location of the Rhp2 protein, immunohistochemistry was performed. IHC staining for Rhp2 occurred along the brush border membrane of the entire lumenal villi, and ISH staining showed Rhp2 mRNA throughout the columnar epithelial cells along the length of the villi in both fed and fasted catsharks (Fig. 2). A two-way

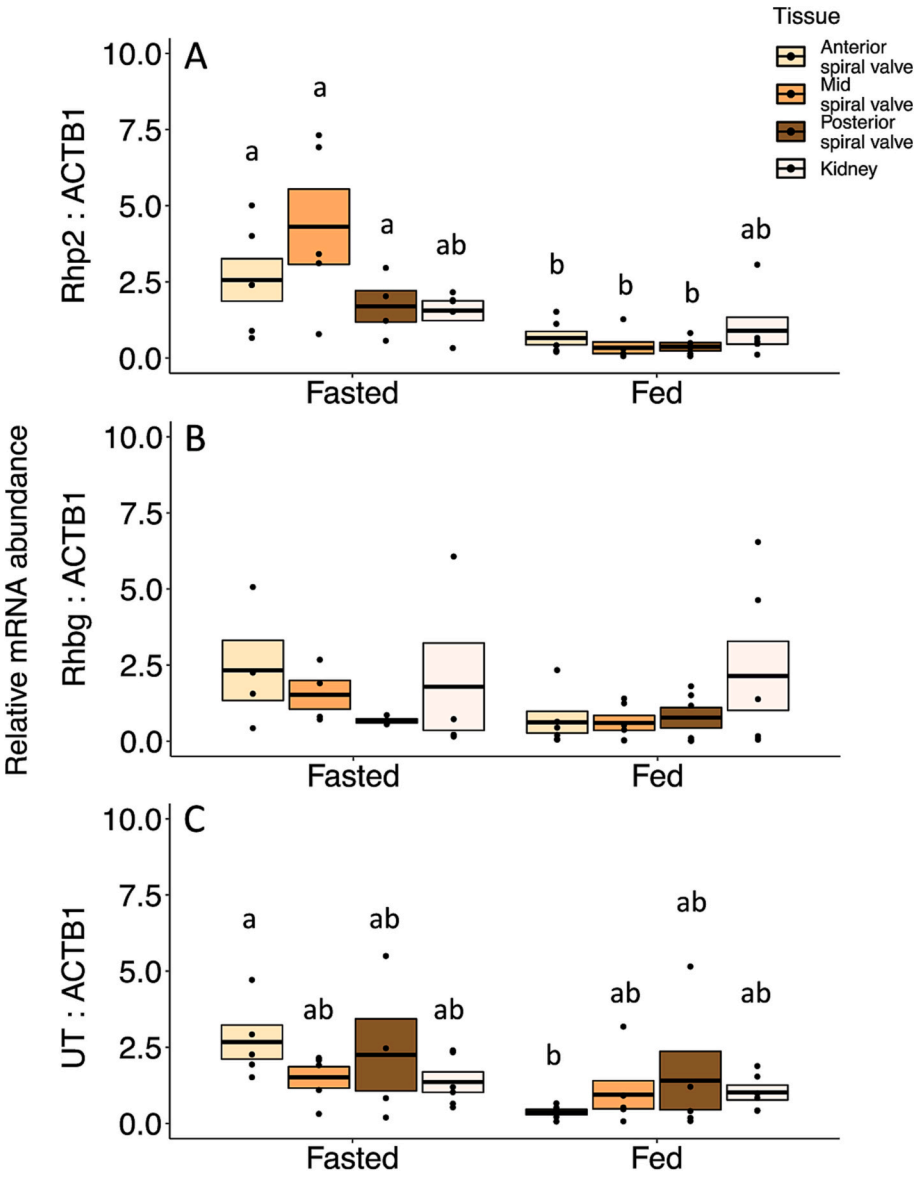

Fig. 1. mRNA abundance of nitrogen transporters A) Rhp2, B) Rhbg, and C) UT, relative to the internal standard reference gene, β-actin (ACTB1), in anterior (yellow box), mid (orange box), and posterior (brown box) intestinal spiral valve regions of cloudy catshark (*Scyliorhinus torazame*), and renal tissue (white boxes). Horizontal line within boxplots indicates mean, and the upper and lower box boundaries indicate sem, with individual data points represented as black dots (n = 5). Means not sharing the same letter are statistically significant. Two-way ANOVA, p < 0.05. (For interpretation of the references to colour in this figure legend, the reader is referred to the web version of this article).

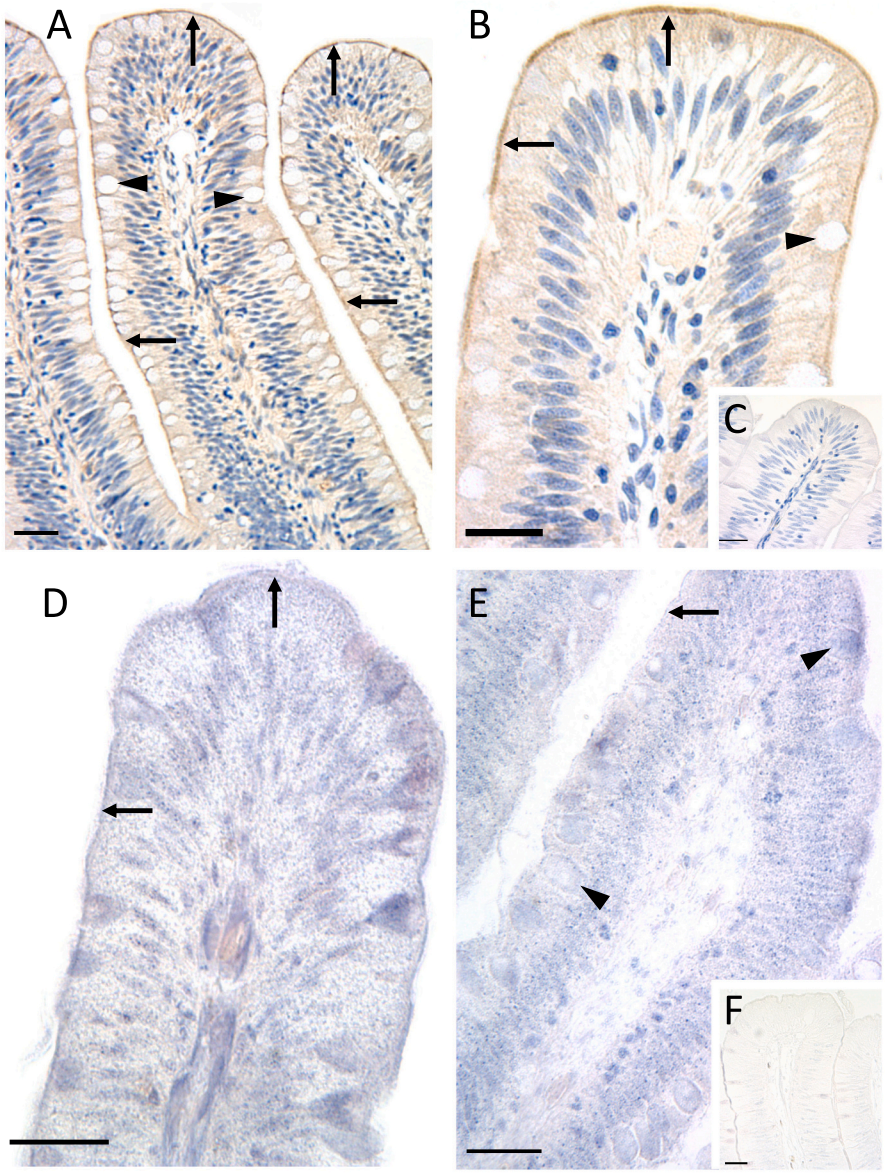

Fig. 2. Intestinal spiral valve villi from cloudy catshark (*Scyliorhinus torazame*). Immunohistochemical protein localization of Rhp2 within spiral valve villi in A) fed and B) fasted catsharks; C) control with no antibody also shown. Bound antibodies were detected with 3,3′-diaminobenzidine (DAB; brown) and counterstained with hematoxylin (blue). *In situ* hybridization of Rhp2 mRNA within D) fed (antisense) and E) fasted (antisense) catsharks; F) control (sense) also shown. Nitro blue tetrazolium (NBT) and bromochloro-indolyl phosphate (BCIP) substrates used for staining. Arrows indicate brush border membrane and arrowheads indicate goblet cells. Bars = 100 μm. (For interpretation of the references to colour in this figure legend, the reader is referred to the web version of this article).

ANOVA was performed to analyze the effects of metabolic state and tissue type on the semi-quantitative determination of protein expression. There was no significant interaction between the effects of metabolic state and tissue type ($F_{2,54} = 0.7$, $p = 0.5$). For metabolic state, there were significantly higher levels of Rhp2 protein expression in all spiral valve regions of the fed catsharks compared to the fasted (anterior, $p < 0.01$; mid, $p < 0.01$; posterior, $p < 0.002$) (Fig. 3). For tissue type, only the posterior spiral valve region of fed catsharks had significantly higher protein expression compared to the anterior region ($p < 0.02$).

3.2. Rhbg

For the mRNA of Rhbg, there was no significant interaction between metabolic state and tissue type ($F_{3,32} = 0.8$, $p = 0.5$). For metabolic state, there were no significant differences between fasted and fed catsharks for any of the spiral valve regions ($p > 0.07$) or kidney ($p = 1.0$). For tissue type, there were no significant differences in mRNA abundance among the tissues of the fasted catsharks ($p > 0.4$), or the fed ($p > 0.9$). (Fig. 1B). ISH staining showed Rhbg mRNA throughout the epithelial cells along the length of the villi in both fed and fasted catsharks (Fig. 4).

3.3. UT

For the mRNA abundance of UT, there was no significant interaction between of metabolic state and tissue type ($F_{3,35} = 1.6$, $p = 0.2$). For metabolic state, there were higher levels of UT mRNA abundance in the anterior spiral valve region of the fasted catshark compared to the fed ($p < 0.001$) (Fig. 1C). For tissue type, there were no significant differences in mRNA abundance among the tissues of the fasted catsharks ($p > 0.4$), or the fed ($p > 0.5$). The specific staining of UT in the renal collecting tubules can be displaced by the addition of excess peptide of the corresponding protein region of UT during the antibody incubation (Fig. 5A,B). With the same condition, displaceable UT signals were found along the basolateral membrane and in the endothelial layer of the blood vessels supplying the spiral valve (Fig. 5C), suggesting a ubiquitous presence of UT within the smooth muscle layer, likely surrounding the capillaries (Fig. 5G). ISH staining also showed UT mRNA ubiquitously present throughout the columnar epithelial cells (Fig. 5I, J).

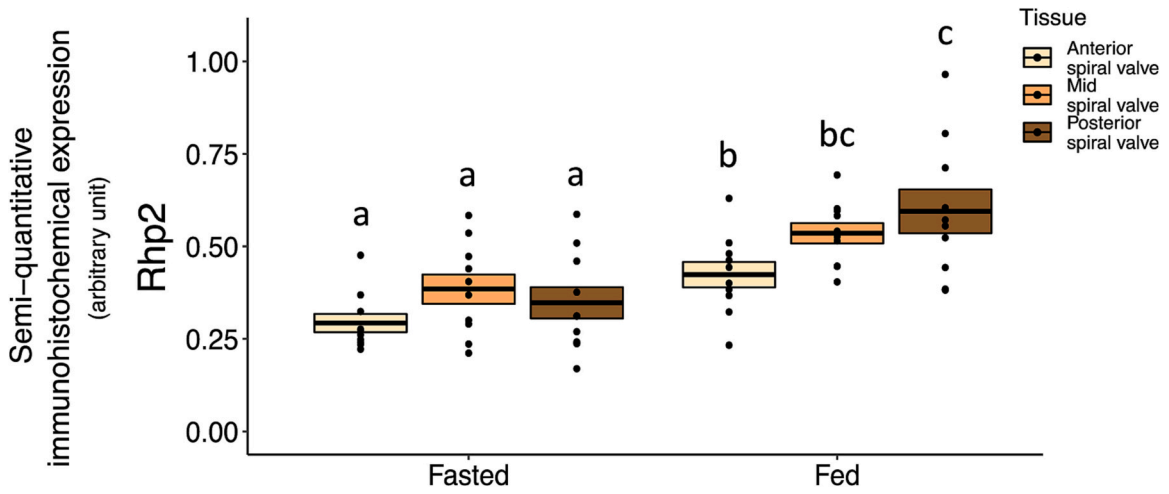

Fig. 3. Semi-quantification of Rhp2 immunohistochemical protein expression within intestinal spiral valve tissues of fed and fasted the cloudy catshark (*Scyliorhinus torazame*). Values (arbitrary) represent protein expression relative to nuclei abundance of ten randomly selected villi within the three spiral valve regions (anterior, yellow boxes; mid, orange boxes; and posterior, brown boxes). Horizontal line within boxplots indicate mean, and the upper and lower box boundaries indicate sem, with individual data points represented as black dots. Means not sharing the same letter as statistically significant. Two-way ANOVA, $p < 0.05$. (For interpretation of the references to colour in this figure legend, the reader is referred to the web version of this article).

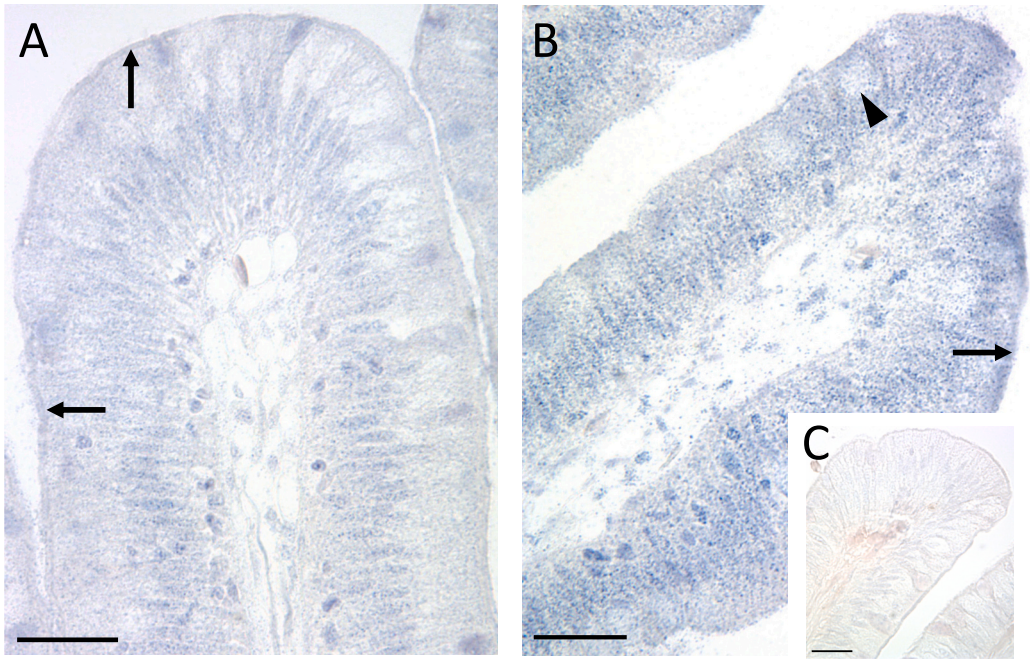

Fig. 4. *In situ* hybridization of Rhbg mRNA within the spiral valve villi of A) fed (antisense) and B) fasted (antisense) cloudy catshark (*Scyliorhinus torazame*); C) control (sense). Arrows indicate brush-border membrane and arrowheads indicate goblet cells. Bars = 100 μm.

3.4. Glutamine Synthetase (GS)

There was no significant interaction between the metabolic state and tissue type ($F_{3,44} = 1.1$, $p = 0.4$) for the mRNA abundance of GS. For metabolic state, there were no significant differences between the fasted and fed catsharks ($p > 0.1$) (Fig. 6A). For tissue type, there were significantly higher levels of the mRNA abundance of GS in the anterior spiral valve region of fasted catshark compared to the mid ($p < 0.001$) and posterior ($p < 0.001$) regions, and the kidney ($p < 0.04$). The posterior spiral valve of the fasted catsharks has significantly lower levels compared to the mid region ($p < 0.02$) and kidney ($p < 0.001$). For fed catsharks, there were significantly lower levels in the posterior spiral valve compared to the anterior ($p < 0.01$), and kidney ($p < 0.04$).

3.5. Carbamoyl phosphate synthetase III (CPS III)

For the mRNA abundance of CPS III, there was no significant interaction between metabolic state and tissue type ($F_{3,44} = 1.3$, $p = 0.3$). For metabolic state, there were no significant differences between the fasted and fed catsharks ($p > 0.1$) (Fig. 6B). For tissue type, there were significantly higher levels of the mRNA abundance of CPS III in the posterior spiral valve of fasted catsharks compared to the anterior ($p < 0.001$) and mid regions ($p < 0.01$). There were also significantly higher levels in the kidney of both the fasted and fed catsharks compared to the three spiral valve regions ($p < 0.05$).

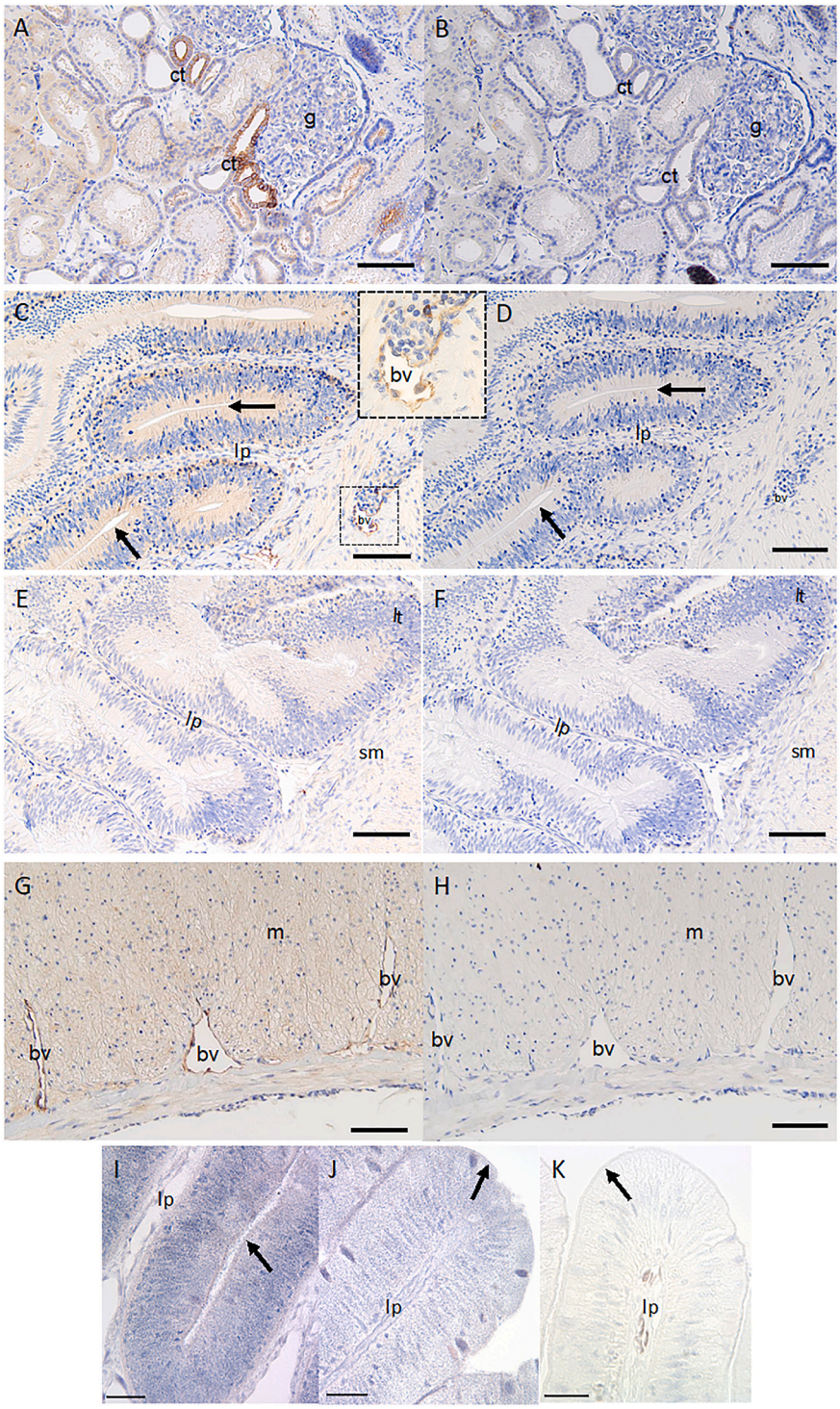

Fig. 5. Immunohistochemical protein localization of UT within the kidney nephron (A-B), and spiral valve villi and smooth muscle (C—H) of cloudy catshark (*Scyliorhinus torazame*). A) kidney; B) kidney control with peptide-blocked antibody used in primary incubation; C) spiral valve villi from fed catshark; D) spiral valve villi control with peptide-blocked antibody used in primary incubation; E) spiral valve villi from fasted catshark; F) spiral valve villi control with peptide-blocked primary antibody; G) spiral valve smooth muscle from fed catshark; H) spiral valve smooth muscle control with peptide-blocked antibody used in primary incubation. Bound antibodies were detected with 3,3′-diaminobenzidine (DAB; brown) and counterstained with hematoxylin (blue). Also shown are *in situ* hybridization of UT mRNA within I) fed (antisense) and J) fasted (antisense) catsharks, and K) control (sense). Nitro blue tetrazolium (NBT) and bromo-chloro-indolyl phosphate (BCIP) substrates used for staining. Arrows indicate brush border membrane. Bars = 100 μm. Abbreviations: bv: blood vessel; ct: collecting tubule; g: glomerulus; lp: lamina propria; lt: lymphoid tissue; m: smooth muscle; sm: submucosa. (For interpretation of the references to colour in this figure legend, the reader is referred to the web version of this article).

3.6. Ornithine transcarbamoylase (OTC)

There was no significant interaction between metabolic state and tissue type ($F_{3,44} = 0.4$, $p = 0.8$) for OTC mRNA abundance. For metabolic state, there were significantly higher levels of OTC mRNA in the mid ($p < 0.01$) and posterior spiral valve ($p < 0.03$), and kidney ($p < 0.04$) of fasted catsharks compared to fed (Fig. 6C). For tissue type, there were no significant differences among the tissues of the fasted catsharks ($p > 0.06$). For fed catsharks, there were significantly higher levels of OTC mRNA abundance in the kidney compared to the mid ($p < 0.01$) and posterior spiral valve ($p < 0.04$).

3.7. Arginase (ARG)

There was no significant interaction between metabolic state and tissue type ($F_{3,44} = 1.2$, $p = 0.3$) for the mRNA abundance of ARG. For metabolic state, there were significantly higher levels of ARG mRNA abundance in the anterior spiral valve of the fasted catsharks compared to the fed ($p < 0.01$), and in the kidney of the fasted catshark compared to the fed ($p < 0.01$) (Fig. 6D). For tissue type, there were significantly higher levels of ARG mRNA abundance in the anterior spiral valve compared to the posterior spiral valve of fasted catsharks ($p < 0.03$), as well as significantly higher levels in the kidney compared to the mid (p

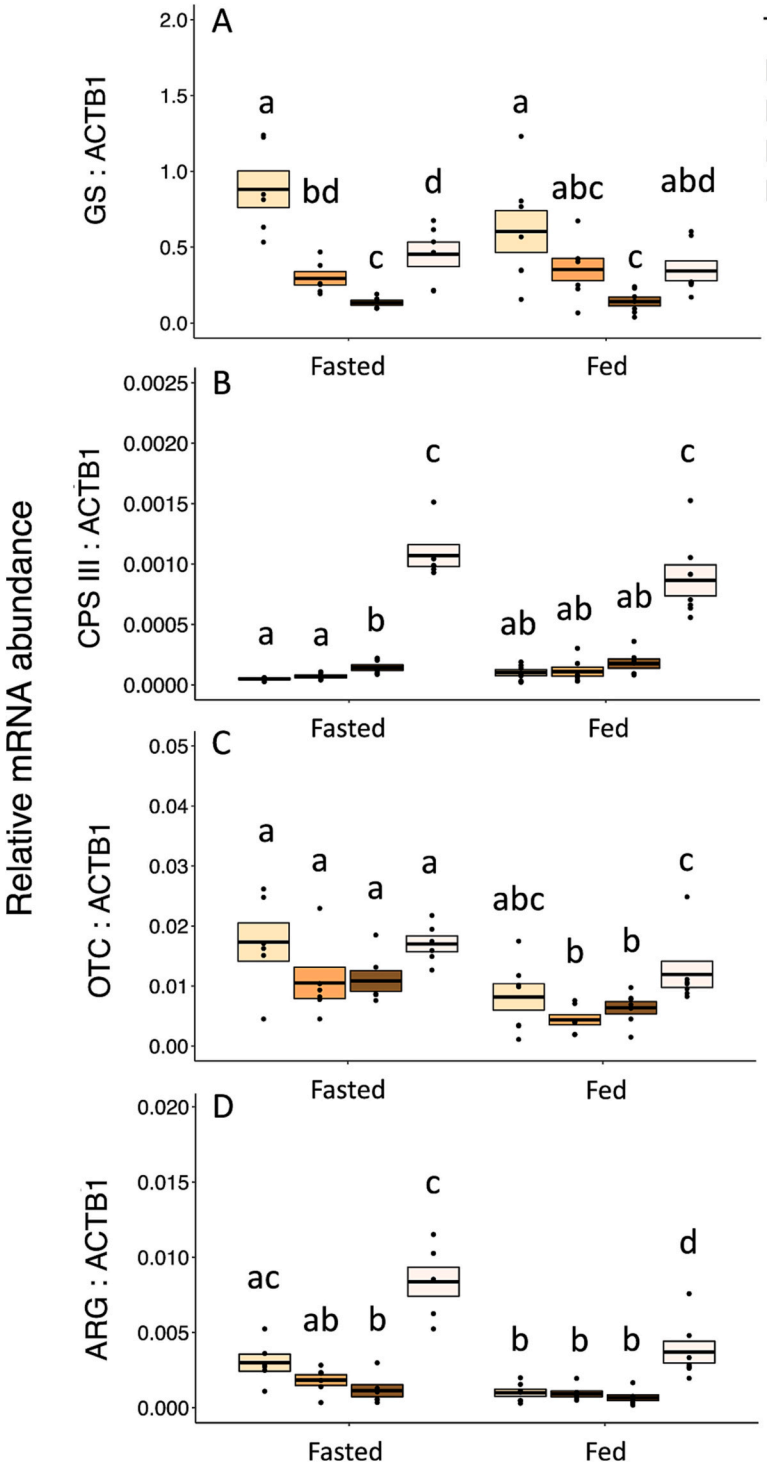

Fig. 6. mRNA abundance of ornithine urea cycle (OUC) enzymes A) GS, glutamine synthetase; B) CPS III, carbamoyl phosphate synthetase III; C) OTC, ornithine transcarbamylase; D) ARG, arginase, relative to the internal standard reference gene, β-actin (ACTB1), in the anterior (yellow box), mid (orange box), and posterior (brown box) intestinal regions of cloudy catsharks (*Scyliorhinus torazame*), and renal tissue (white boxes). Horizontal line within boxplots indicates mean, and the upper and lower box boundaries indicate sem, with individual data points represented as black dots ($n = 5$). Means not sharing the same letter are statistically significant. Two-way ANOVA, $p < 0.05$. (For interpretation of the references to colour in this figure legend, the reader is referred to the web version of this article).

< 0.01) and posterior spiral valve ($p < 0.001$). In fed catsharks, the ARG mRNA abundance was significantly increased in the kidney compared to all three spiral valve regions ($p < 0.001$).

4. Discussion

This study demonstrated the presence of two Rh glycoprotein ammonia transporters (Rhp2, Rhbg) and a urea transporter (UT) within the intestinal and renal tissues of the cloudy catshark, as well as the mRNA of four OUC enzymes (GS, CPS III, OTC, ARG). There was a significant increase in mRNA abundance of Rhp2 in all three spiral valve regions of the fasted catsharks compared to the fed, but no significant differences along the length of the spiral valve for either the fasted or the fed catsharks (Fig. 1A). In contrast, the protein expression of Rhp2 was significantly higher in all three spiral valve regions of the fed catsharks compared to the fasted, as well as higher levels in the posterior spiral valve of the fed catsharks compared to the anterior (Fig. 3). It is known that transcript abundance is not enough to predict protein expression levels (for reviews on this see de Sousa Abreu et al., 2009, Liu et al., 2016, and McManus et al., 2015). Regulation of gene expression is dependent upon many factors, including the rates of transcription, translation, and degradation, the availability of resources necessary to

synthesize the proteins, or the half-life of mRNA (median: 9 h) compared to protein (median: 46 h) (de Sousa Abreu et al., 2009; Liu et al., 2016; McManus et al., 2015; Schwanhüusser et al., 2011). Therefore, there may be unresolved factors not explored in this study that were responsible for the demonstrated differences between the transcript abundance if Rhp2 and the protein expression. It is also possible that the higher levels of protein expression in the fed catsharks were due to a greater trafficking of the Rhp2 protein from the cytoplasm or submembrane regions to the apical membrane, rather than an increase in protein synthesis. The mobilization of the Rhp2 protein to the apical membrane is likely linked to the digestion of food and the subsequent uptake of ammonia from the lumen, as evidenced by the IHC staining showing that Rhp2 was localized at the brush border membrane of the intestinal villi (Fig. 2A, B). This apical protein expression is in contrast to the basolateral localization in the kidney tubules of *T. scyllium* (Nakada et al., 2010). The apical location of Rhp2 protein expression along the intestinal villi would suggest it plays a role in the absorption of ammonia from the lumen into the epithelia for the purpose of nitrogen recruitment.

Once uptake into the epithelial cells occurs, ammonia can be used to synthesize glutamine, the nitrogen-donating substrate for the OUC (Anderson, 1991). The activity of three OUC enzymes (CPS III, OTC, ARG) have previously been demonstrated within the intestinal tissues of the spiny dogfish (Kajimura et al., 2006), indicating ammonia within the epithelia, possibly taken-up by Rhp2, could be used for the production of urea. Our study quantified the mRNA abundance of GS, CPS III, OTC, ARG within the intestinal and renal tissues of the cloudy catshark (Fig. 6). The mRNA abundance of GS was orders of magnitude higher than the other three enzymes, while CPS III and ARG had the lowest levels. This is likely due to the use of glutamine as an important fuel source in these animals (Chamberlin and Ballantyne, 1992), as well as being used as a precursor of urea synthesis (Anderson, 1991). There were some differences in the mRNA abundance of all of the OUC enzymes along the length of the spiral valve. GS abundance was lowest in the posterior region compared to the anterior of both fed and fasted catsharks. In fasted catsharks, CPS III abundance was higher in the posterior spiral valve compared to the anterior, but not in fed catsharks. There were no differences in OTC abundance among all spiral valve regions. ARG had the lowest levels in the posterior spiral valve of fasted catsharks compared to the anterior, but no regional differences were found in the fed animals. In comparison, the spiral valve of the spiny dogfish had no significant differences in the activity of the four enzymes between fasted and fed animals (Kajimura et al., 2006), but regional differences across the spiral valve regions were not investigated. The mRNA abundance of these enzymes, as well as the enzyme activity reported by Kajimura et al. (2006) indicate the synthesis of urea occurs within the intestinal tissues of marine elasmobranchs. As there is no common trend in transcript abundance among the four enzymes it is currently not possible to identify which region, if any, contributes more to the synthesis of urea in the cloudy catshark under these conditions.

We also demonstrated the mRNA abundance of all four OUC enzymes within the renal tissue of the catshark (Fig. 6). In mammals, CPS I (the mammalian equivalent to CPS III), OTC, and ARG have been identified within renal tissues of rat (Aperia et al., 1979) and dog (Von Dreele and Banks, 1985). Even though the mammalian kidney is designed to eliminate waste nitrogen as urea, urea can also be retained within the inner medulla to prevent osmotic diuresis; indeed, it was demonstrated that the presence of UTs within the renal tissue of mice work to concentrate the urine (Fenton et al., 2004; Fenton and Knepper, 2007; Geng et al., 2020). Additionally, the presence of the OUC enzymes in the renal tissue of rats has been attributed to the role that urea plays in concentrating urine (Aperia et al., 1979). In contrast, marine elasmobranch kidneys are designed to reabsorb and retain filtered urea (Boylan, 1972; Boylan, 1967; Hyodo et al., 2014; Hyodo et al., 2004; Kempton, 1953). In the elephant shark, *in situ* hybridization showed the mRNA of GS, OTC, and Rhp2 were all located in the same tubular segment of the kidney sinus zone (Hyodo et al., 2014). Therefore, urinary ammonia may be taken-up into the tubule epithelium by Rhp2, and used to synthesize urea via the OUC (Hyodo et al., 2014) and subsequently moved into the plasma for circulation as a mechanism to retain nitrogen and use for whole-body nitrogen balance.

The mRNA levels of Rhbg in the spiral valve and renal tissues did not differ between fasted and fed catsharks, nor between any of the spiral valve regions and the kidney (Figs. 1, 4). We did not have a verified system to determine the localization of Rhbg through IHC; however, Rhbg expression has been located along the basolateral membrane of fish branchial epithelia (Wright and Wood, 2009), mammalian renal tubules, and hepatic tissue (Verlander et al., 2003; Weiner et al., 2003). If the same basolateral pattern persists in the spiral valve, Rhbg may facilitate the transport of ammonia across the basolateral membrane to the plasma for subsequent transport to the liver and/or skeletal muscle, which are known locations of urea production via the OUC (Casey and Anderson, 1982; Kajimura et al., 2006; Steele et al., 2005). The ISH staining for Rhbg and Rhp2 indicates the mRNA of both ammonia transporters occurs throughout the intestinal epithelia (Figs. 2D,E and 4A,B). Therefore, it is reasonable to speculate that ammonia may be taken up from the intestinal lumen by apically located Rhp2 along the brush border membrane and transported to the blood by Rhbg on the basolateral membrane.

Immunohistological staining showed UT expression along the basolateral membrane and blood vessels of the spiral valve (Fig. 5C,E), suggesting that it is involved in the transport of urea between the intestinal epithelial cells and the plasma. When combined with the Rhp2 apical localization and the presence of the OUC enzymes, as demonstrated by our transcript abundance data and previous enzyme activity work (Kajimura et al., 2006), we suggest ammonia within the spiral valve can be taken-up by Rhp2 along the brush border membrane and shuttled to the OUC within the epithelium for urea synthesis. The resulting urea is then subsequently moved across the basolateral membrane to the blood vessels via the UT.

The IHC staining for the renal UT showed expression in the collecting tubules (Fig. 5A), as seen in the banded houndshark (Hyodo et al., 2014; Hyodo et al., 2004), and the renal UT mRNA abundance did not differ between fasted and fed catsharks (Fig. 1C). More than 90% of urea filtered from the primary urine is reabsorbed by elasmobranch kidney (Boylan, 1972; Boylan, 1967; Hyodo et al., 2004; Kempton, 1953), likely aided by renal UTs. For these nitrogen-limited animals, the retention of urea at the kidney reduces the metabolic cost of synthesizing urea, which has been calculated to require five molecules of ATP for every molecule of urea synthesized (Walsh and Mommsen, 2001). Identification of a UT in both the apical and basolateral epithelial membranes of the collecting tubule in the renal tissue of *T. scyllium* suggests this area is responsible for the reabsorption of urea from the urine (Hyodo et al., 2004). The increased UT mRNA abundance in fasted catsharks could be linked to an increase in urea reabsorption during times of reduced exogenous urea intake, likely to aid in maintaining a continual supply of nitrogen for whole-body homeostasis.

5. Conclusions

This study demonstrated the presence of three nitrogen transporters (Rhp2, Rhbg, UT) within the intestinal and renal tissues of the cloudy catshark, and highlighted the importance of nitrogen trafficking and retention within these tissues. This is the first study to identify the cellular localization of Rhp2 along the apical brush border membrane, and UT along the basolateral membrane and blood vessels in the spiral valve of a marine elasmobranch. Rhp2 along the brush border membrane suggests it is involved in ammonia uptake from the lumen into the epithelial cells. The mRNA of the OUC enzymes suggests that urea is synthesized within the intestinal epithelium, and possibly within the renal tissues as well, with both tissues likely contributing to the whole-body nitrogen budget for these animals. The basolateral and blood vessel

localization of UT suggests it may be involved in the uptake of urea from the intestinal epithelium into the plasma. The presence of both Rhp2 and Rhbg along the spiral valve highlights the importance of ammonia trafficking for these ureotelic animals, as a method of nitrogen recruitment for both metabolic and osmoregulatory purposes.

Funding

Research was supported by Natural Sciences and Engineering Research Council of Canada (NSERC) Discovery Grant to W.G.A (05348). J.L.H. was supported by NSERC Alexander Graham Bell Canada Graduate Scholarship – D, and the NSERC Michael Smith Foreign Study Supplement.

Declaration of Competing Interest

The authors declare no conflicts.

Data availability

Data will be made available on request.

Acknowledgements

We acknowledge the University of Manitoba campuses are located on the original lands of Anishinaabeg, Cree, Oji-Cree, Dakota, and Dene peoples, and on the homeland of the Métis Nation. We thank Dr. Wataru Takagi and Naotaka Aburatani for their help with processing samples in the lab, as well as all members of the AORI Physiology laboratory for help with shark care and maintenance.

Appendix A. Supplementary data

Supplementary data to this article can be found online at https://doi.org/10.1016/j.cbpa.2023.111418.

References

Anderson, P.M., 1980. Glutamine- and N-acetylglutamate-dependent carbamoyl phosphate synthetase in elasmobranchs. Science 208, 291–293.

Anderson, P.M., 1991. Glutamine-dependent urea synthesis in elasmobranch fishes. Biochem. Cell Biol. 69, 317–319. https://doi.org/10.1139/o91-049.

Anderson, W.G., Dasiewicz, P.J., Liban, S., Ryan, C., Taylor, J.R., Grosell, M., Weihrauch, D., 2010. Gastro-intestinal handling of water and solutes in three species of elasmobranch fish, the white-spotted bamboo shark, *Chiloscyllium plagiosum*, little skate, *Leucoraja erinacea* and the clear nose skate *Raja eglanteria*. Comp. Biochem. Physiol. A 155, 493–502. https://doi.org/10.1016/j.cbpa.2009.09.020.

Anderson, W.G., McCabe, C., Brandt, C., Wood, C.M., 2015. Examining urea flux across the intestine of the spiny dogfish, *Squalus acanthias*. Comparative Biochemistry and Physiology Part A: Molecular & Integrative Physiology 181, 71–78. https://doi.org/10.1016/j.cbpa.2014.11.023.

Aperia, A., Broberger, O., Larsson, A., Snellman, K., 1979. Studies of renal urea cycle enzymes. I. Renal concentrating ability and urea cycle enzymes in the rat during protein deprivation. Scand. J. Clin. Lab. Invest. 39, 329–336. https://doi.org/10.3109/00365517909106116.

Boylan, J.W., 1967. Gill permeability in *Squalus acanthias*. In: Gilbert, P., Mathewson, R., Rall, D. (Eds.), Sharks, Skates, and Rays: The Biology of Elasmobranch Fishes, pp. 197–206.

Boylan, J.W., 1972. A model for passive urea reabsorption in the elasmobranch kidney. Comp. Biochem. Physiol. A 42A, 27–30. https://doi.org/10.1016/0300-9629(72)90361-1.

Bucking, C., 2015. Feeding and digestion in elasmobranchs: tying diet and physiology together. In: *Fish physiology*, (Vol. 34,. Academic Press, pp. 347–394. https://doi.org/10.1016/B978-0-12-801286-4.00006-X.

Casey, C.A., Anderson, P.M., 1982. Subcellular location of glutamine synthetase and urea cycle enzymes in liver of spiny dogfish (*Squalus acanthias*). J. Biol. Chem. 257, 8449–8453.

Chamberlin, M.E., Ballantyne, J.S., 1992. Glutamine metabolism in elasmobranch and agnathan muscle. J. Exp. Zool. 264, 267–272. https://doi.org/10.1002/jez.1402640306.

Crowe, A., Yue, W., 2019. Semi-quantitative determination of protein expression using immunohistochemistry staining and analysis: an integrated protocol. Bio-Protocol 9, 1–11. https://doi.org/10.21769/bioprotoc.3465.

Crowe, A., Zheng, W., Miller, J., Pahwa, S., Alam, K., Fung, K.M., Rubin, E., Yin, F., Ding, K., Yue, W., 2019. Characterization of plasma membrane localization and phosphorylation status of organic anion transporting polypeptide (OATP) 1B1 c.521 T>C nonsynonymous single-nucleotide polymorphism. Pharm. Res. 36 https://doi.org/10.1007/s11095-019-2634-3.

de Sousa Abreu, R., Penalva, L.O., Marcotte, E.M., Vogel, C., 2009. Global signatures of protein and mRNA expression levels. Mol. BioSyst. 5, 1512–1526. https://doi.org/10.1039/b908315d.

Fenton, R.A., Knepper, M.A., 2007. Urea and renal function in the 21st century: insights from knockout mice. J. Am. Soc. Nephrol. 18, 679–688. https://doi.org/10.1681/ASN.2006101108.

Fenton, R.A., Chou, C.L., Stewart, G.S., Smith, C.P., Knepper, M.A., 2004. Urinary concentrating defect in mice with selective deletion of phloretin-sensitive urea transporters in the renal collecting duct. Proc. Natl. Acad. Sci. U. S. A. 101, 7469–7474. https://doi.org/10.1073/pnas.0401704101.

Geng, X., Zhang, S., He, J., Ma, A., Li, Y., Li, M., Zhou, H., Chen, G., Yang, B., 2020. The urea transporter UT-A1 plays a predominant role in a urea-dependent urine-concentrating mechanism. J. Biol. Chem. 295, 9893–9900. https://doi.org/10.1074/jbc.ra120.013628.

Hara, Y., Yamaguchi, K., Onimaru, K., Kadota, M., Koyanagi, M., Keeley, S.D., Tatsumi, K., Tanaka, K., Motone, F., Kageyama, Y., Nozu, R., Adachi, N., Nishimura, O., Nakagawa, R., Tanegashima, C., Kiyatake, I., Matsumoto, R., Murakumo, K., Nishida, K., Terakita, A., Kuratani, S., Sato, K., Hyodo, S., Kuraku, S., 2018. Shark genomes provide insights into elasmobranch evolution and the origin of vertebrates. Nat. Ecol. Evol. 2, 1761–1771. https://doi.org/10.1038/s41559-018-0673-5.

Hoogenboom, J.L., Weinrauch, A.M., Wood, C.M., Anderson, W.G., 2020. The effects of digesting a urea-rich meal on North Pacific spiny dogfish (*Squalus acanthias suckleyi)*. Comp. Biochem. Physiol. A 249, 110775. https://doi.org/10.1016/j.cbpa.2020.110775.

Hyodo, S., Katoh, F., Kaneko, T., Takei, Y., 2004. A facilitative urea transporter is localized in the renal collecting tubule of the dogfish *Triakis scyllia*. J. Exp. Biol. 207, 347–356. https://doi.org/10.1242/jeb.00773.

Hyodo, S., Kakumura, K., Takagi, W., Hasegawa, K., Yamaguchi, Y., 2014. Morphological and functional characteristics of the kidney of cartilaginous fishes: with special reference to urea reabsorption. Am. J. Physiol. - Regul. Integr. Comp. Physiol. 307, R1381–R1395. https://doi.org/10.1152/ajpregu.00033.2014.

Janech, M.G., Fitzgibbon, W.R., Chen, R., Nowak, M.W., Miller, D.H., Paul, R.V., Ploth, D.W., 2003. Molecular and functional characterization of a urea transporter from the kidney of the Atlantic stingray. Am. J. Physiol. Ren. Physiol. 284, F996–F1005. https://doi.org/10.1152/ajprenal.00174.2002.

Janech, M.G., Gefroh, H.A., Cwengros, E.E., Sulikowski, J.A., Ploth, D.W., Fitzgibbon, W. R., 2008. Cloning of urea transporters from the kidneys of two batoid elasmobranchs: evidence for a common elasmobranch urea transporter isoform. Mar. Biol. 153, 1173–1179. https://doi.org/10.1007/s00227-007-0889-4.

Kajimura, M., Walsh, P.J., Mommsen, T.P., Wood, C.M., 2006. The dogfish shark (*Squalus acanthias*) increases both hepatic and extrahepatic ornithine urea cycle enzyme activities for nitrogen conservation after feeding. Physiol. Biochem. Zool. 79, 602–613.

Kakumura, K., Watanabe, S., Bell, J.D., Donald, J.A., Toop, T., Kaneko, T., Hyodo, S., 2009. Multiple urea transporter proteins in the kidney of holocephalan elephant fish (*Callorhinchus milii*). Comp. Biochem. Physiol. - B Biochem. Mol. Biol. 154, 239–247. https://doi.org/10.1016/j.cbpb.2009.06.009.

Kempton, R.T., 1953. Studies on the elasmobranch kidney. II. Reabsorption of urea by the smooth dogfish, Mustelus canis. Biol. Bull. 104 (1), 45–56.

Lawrence, M.J., 2014. Functional Characterization of Renal ammonia Transport and Acid-Base Regulation in Teleost and Elasmobranch Fishes. McMaster University, Hamilton, ON.

Liew, H.J., De Boeck, G., Wood, C.M., 2013. An *in vitro* study of urea, water, ion and CO2/HCO3- transport in the gastrointestinal tract of the dogfish shark (*Squalus acanthias*): the influence of feeding. J. Exp. Biol. 216, 2063–2072. https://doi.org/10.1242/jeb.082313.

Liu, Y., Beyer, A., Aebersold, R., 2016. On the dependency of cellular protein levels on mRNA abundance. Cell 165, 535–550. https://doi.org/10.1016/j.cell.2016.03.014.

Marini, A.-M., Matassi, G., Raynal, V., André, B., Cartron, J.-P., Chérif-Zahar, B., 2000. The human Rhesus-associated RhAG protein and a kidney homologue promote ammonium transport in yeast. Nat. Genet. 26, 341–344. https://doi.org/10.1038/81656.

McManus, J., Cheng, Z., Vogel, C., 2015. Next-generation analysis of gene expression regulation - comparing the roles of synthesis and degradation. Mol. BioSyst. 11, 2680–2689.

Mistry, A.C., Chen, G., Kato, A., Nag, K., Sands, J.M., Hirose, S., 2005. A novel type of urea transporter, UT-C, is highly expressed in proximal tubule of seawater eel kidney. Am. J. Physiol. Ren. Physiol. 288, 455–465. https://doi.org/10.1152/ajprenal.00296.2004.

Morgan, R.L., Wright, P.A., Ballantyne, J.S., 2003. Urea transport in kidney brush-border membrane vesicles from an elasmobranch, *Raja erinacea*. J. Exp. Biol. 206, 3293–3302. https://doi.org/10.1242/Jeb.00555.

Nakada, T., Westhoff, C.M., Yamaguchi, Y., Hyodo, S., Li, X., Muro, T., Kato, A., Nakamura, N., Hirose, S., 2010. Rhesus glycoprotein P2 (Rhp2) is a novel member of the Rh family of ammonia transporters highly expressed in shark kidney. J. Biol. Chem. 285, 2653–2664. https://doi.org/10.1074/jbc.M109.052068.

Nawata, C.M., Walsh, P.J., Wood, C.M., 2015a. Nitrogen metabolism, acid–base regulation, and molecular responses to ammonia and acid infusions in the spiny dogfish shark (*Squalus acanthias*). J. Comp. Physiol. B. 185, 511–525. https://doi.org/10.1007/s00360-015-0898-4.

Nawata, C.M., Walsh, P.J., Wood, C.M., 2015b. Physiological and molecular responses of the spiny dogfish shark (*Squalus acanthias*) to high environmental ammonia: scavenging for nitrogen. J. Exp. Biol. 218, 238–248. https://doi.org/10.1242/jeb.114967.

R Core Team, 2017. R: A Language and Environment for Statistical Computing. R Foundation for Statistical Computing, Vienna, Austria, p. 2017.

Schooler, J.M., Goldstein, L., Hartman, S.C., Forster, R.P., 1966. Pathways of urea synthesis in the elasmobranch, *Squalus acanthias*. Comp. Biochem. Physiol. 18, 271–281.

Schwanhüusser, B., Busse, D., Li, N., Dittmar, G., Schuchhardt, J., Wolf, J., Chen, W., Selbach, M., 2011. Global quantification of mammalian gene expression control. Nature 473, 337–342. https://doi.org/10.1038/nature10098.

Shayakul, C., Hediger, M.A., 2004. The SLC14 gene family of urea transporters. Pflugers Arch. Eur. J. Physiol. 447, 603–609. https://doi.org/10.1007/s00424-003-1124-x.

Shayakul, C., Clémençon, B., Hediger, M.A., 2013. The urea transporter family (SLC14): physiological, pathological and structural aspects. Mol. Asp. Med. 34, 313–322. https://doi.org/10.1016/j.mam.2012.12.003.

Smith, H.W., 1936. The retention and physiological role of urea in the elasmobranchii. Biol. Rev. 11, 49–82. https://doi.org/10.1111/j.1469-185X.1936.tb00497.x.

Smith, C.P., Wright, P.A., 1999. Molecular characterization of an elasmobranch urea transporter. Am. Physiol. Soc. - Regul. Integr. Comp. Physiol. 276, R622–R626. https://doi.org/10.1016/S0016-5085(77)80340-5.

Steele, S.L., Yancey, P.H., Wright, P.A., 2005. The little skate *Raja erinacea* exhibits an extrahepatic ornithine urea cycle in the muscle and modulates nitrogen metabolism during low-salinity challenge. Physiol. Biochem. Zool. 78, 216–226.

Takabe, S., Teranishi, K., Takaki, S., Kusakabe, M., Hirose, S., Kaneko, T., Hyodo, S., 2012. Morphological and functional characterization of a novel Na +/K+-ATPase-immunoreactive, follicle-like structure on the gill septum of Japanese banded houndshark, *Triakis scyllium*. Cell Tissue Res. 348, 141–153. https://doi.org/10.1007/s00441-012-1344-5.

Takagi, W., Kajimura, M., Bell, J.D., Toop, T., Donald, J.A., Hyodo, S., 2012. Hepatic and extrahepatic distribution of ornithine urea cycle enzymes in holocephalan elephant fish (*Callorhinchus milii*). Comp. Biochem. Physiol. - B Biochem. Mol. Biol. 161, 331–340. https://doi.org/10.1016/j.cbpb.2011.12.006.

Takagi, W., Kajimura, M., Tanaka, H., Hasegawa, K., Ogawa, S., Hyodo, S., 2017. Distributional shift of urea production site from the extraembryonic yolk sac membrane to the embryonic liver during the development of cloudy catshark (*Scyliorhinus torazame*). Comp. Biochem. Physiol. A 211, 7–16. https://doi.org/10.1016/j.cbpa.2017.05.019.

Verlander, J.W., Miller, R.T., Frank, A.E., Royaux, I.E., Kim, Y.H., Weiner, I.D., 2003. Localization of the ammonium transporter proteins RhBG and RhCG in mouse kidney. Am. J. Physiol. Ren. Physiol. 284, 323–337. https://doi.org/10.1152/ajprenal.00050.2002.

Von Dreele, M.M., Banks, R.O., 1985. Urea synthesis in the canine kidney. Kidney Blood Press Res. 8, 73–79. https://doi.org/10.1159/000173038.

Walsh, P.J., Mommsen, T.P., 2001. Evolutionary considerations of nitrogen metabolism and excretion. In: Wright, P.A., Anderson, P.M. (Eds.), Fish Physiology: Nitrogen Excretion. Academic Press, New York, pp. 1–30.

Weiner, I.D., Miller, R.T., Verlander, J.W., 2003. Localization of the ammonium transporters, Rh B glycoprotein and Rh C glycoprotein, in the mouse liver. Gastroenterology 124, 1432–1440. https://doi.org/10.1016/S0016-5085(03)00277-4.

Wickham, H., 2009. ggplot2: Elegant Graphics for Data Analysis.

Wood, C.M., Giacomin, M., 2016. Feeding through your gills and turning a toxicant into a resource: how the dogfish shark scavenges ammonia from its environment. J. Exp. Biol. 219, 3218–3226. https://doi.org/10.1242/jeb.145268.

Wood, C.M., Kajimura, M., Bucking, C., Walsh, P.J., 2007. Osmoregulation, ionoregulation and acid–base regulation by the gastrointestinal tract after feeding in the elasmobranch (*Squalus acanthias*). J. Exp. Biol. 210 (8), 1335–1349. https://doi.org/10.1242/jeb.02736.

Wood, C.M., Kajimura, M., Mommsen, T.P., Walsh, P.J., 2005. Alkaline tide and nitrogen conservation after feeding in an elasmobranch (*Squalus acanthias*). J. Exp. Biol. 208 (14), 2693–2705. https://doi.org/10.1242/jeb.01678.

Wood, C.M., Liew, H.J., De Boeck, G., Hoogenboom, J.L., Anderson, W.G., 2019. Nitrogen handling in the elasmobranch gut: a role for microbial urease. J. Exp. Biol. 222, jeb194787. https://doi.org/10.1242/jeb.194787.

Wright, P.A., 1995. Nitrogen excretion: three end products, many physiological roles. The J. Exp. Biol. 198 (2), 273–281. https://doi.org/10.1242/jeb.198.2.273.

Wright, P.A., Wood, C.M., 2009. A new paradigm for ammonia excretion in aquatic animals: role of Rhesus (Rh) glycoproteins. J. Exp. Biol. 212, 2303–2312. https://doi.org/10.1242/jeb.023085.

Yamaguchi, Y., Takaki, S., Hyodo, S., 2009. Subcellular distribution of urea transporter in the collecting tubule of shark kidney is dependent on environmental salinity. J. Exp. Zool. Part A 311, 705–718. https://doi.org/10.1002/jez.558.

You, G., Smith, C.P., Kanal, Y., Lee, W., Stelzner, M., Hediger, M.A., 1993. Cloning and characterization of the vasopressin-regulated urea transporter. Nature 365, 844–847.